South China Sea Warm Pool in Boreal Spring

Peter C. Chu and *C.-P. Chang*
Naval Postgraduate School, Monterey, CA 93943, USA, October 23, 1996
Received November 6, 1996

ABSTRACT

During the boreal spring of 1966, a warm-core eddy is identified in the upper South China Sea (SCS) west of the Philippines through an analysis of the U.S. Navy's Master Oceanographic Observation Data Set. This eddy occurred before the development of the northern summer monsoon and disappeared afterward. We propose that this eddy is a result of the radiative warming during spring and the downwelling due to the anticyclonic forcing at the surface. Our hypothesis suggests an air-sea feedback scenario that may explain the development and withdrawal of the summer monsoon over the SCS. The development phase of the warm-core eddy in this hypothesis is tested by using the Princeton Ocean model.

Key words: Warm-core eddy, Summer monsoon, Downwelling, South China Sea

1. INTRODUCTION

The South China Sea (SCS) has a bottom topography (Figure 1) that makes it a unique semi-enclosed ocean basin. Extended continental shelves (less than 100 m deep) are found on the western and southern parts, while steep slopes with almost no shelves are found in the eastern part of SCS. The deepest water is confined to a bowl-type trench with the maximum depth around 4,700 m. This semi-enclosed deep ocean basin is overlaid by a pronounced monsoonal surface wind whose direction reverses from northeast in the Northern winter to southwest in the Northern summer. The purpose of this work is to discuss a possible atmosphere-ocean interaction between the monsoonal surface wind and the upper layer of the SCS, based on the observation of a warm pool during the Northern spring.

Based on limited data sets, both cool and warm pools have been observed in the SCS. Dale (1956) and Uda and Nakao (1974) reported a cool pool off the central Vietnamese Coast in summer. Nitan (1970) found a cool pool located to the northwest of Luzon. Reports from the South China Sea Institute of Oceanology (SCSIO, 1985) indicate that in the central SCS, a warm pool appears in both summer and winter, but more closer in Vietnam in summer at the surface. A cool pool was detected in the central SCS during 29 December 1993 to 5 January 1994 from the analysis of TOPEX / Poseidon data (Soong, et al., 1995).

The availability of the long-term U.S. Navy's Master Observational Oceanographic Data Set (MOODS) made it possible to analyze the upper ocean thermal structure over several extended periods (Chu, et al., 1996). Careful hand analysis for Spring of 1966, during the high of the Vietnam War when ship observations were abundant, revealed the existence of a warm pool in the central SCS. The observation results motivated us to propose a hypothesis of combined wind-topographic effects for the formation of this boreal spring warm pool. This hypothesis was then tested with a three-dimensional ocean circulation model simulation.

II. MASTER OCEANOGRAPHIC OBSERVATION DATA SET (MOODS)

The MOODS is a compilation of ocean data observed worldwide consisting of (a) temperature-only profiles; (b) both temperature and salinity profiles, (c) sound-speed profiles, and (d) surface temperature (drifting buoy). These measurements are, in general, irregular in time and space. Due to the shear size (more than six million profiles total for the global ocean) and constant influx of data to NAVOCEANO from various sources, quality control is very important. The primary editing procedure included removal of profiles with obviously erroneous location, profiles with large spikes (temperature higher than 35°C and lower than −2°C), and profiles displaying features that do not match the characteristics of surrounding profiles such as profiles showing increase of temperature with depth. After quality control, the historical MOODS data (1900–1995) consisted of 189,059 profiles for the whole SCS (5°S–25°N, 105°–120°E). The temporal and spatial distributions of MOODS stations (Figure 2) are irregular. The distributions of the MOODS stations for 1968 (maximum number of observations) and for 1984 (minimum number of observations) are shown in Figure 3.

To investigate the transient features of the SCS thermal structure, the data base was binned for three ten-day periods each month (the last bin each month includes 8–11 days depending on the calendar). The temporal distribution of the number of profiles (Figure 3) indicates that the most dense observations were obtained during the high period of the Vietnamese War (1965–1969). In contrast to the large variations of the number of observa-

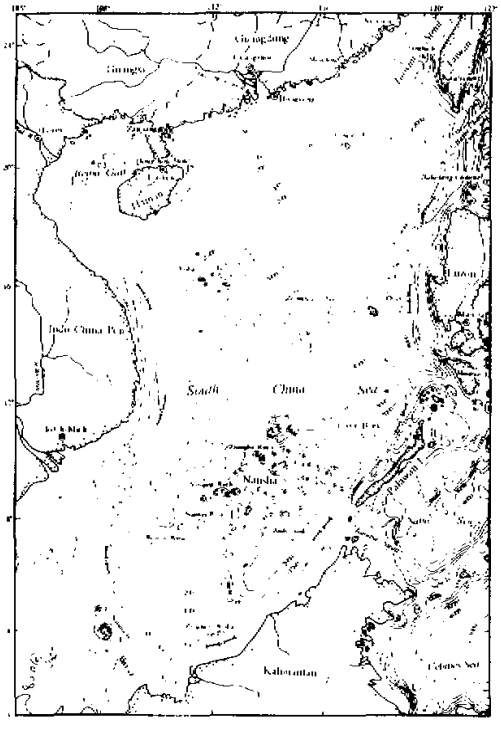

Fig. 1. Geography and isobaths showing the bottom topography of the South China Sea.

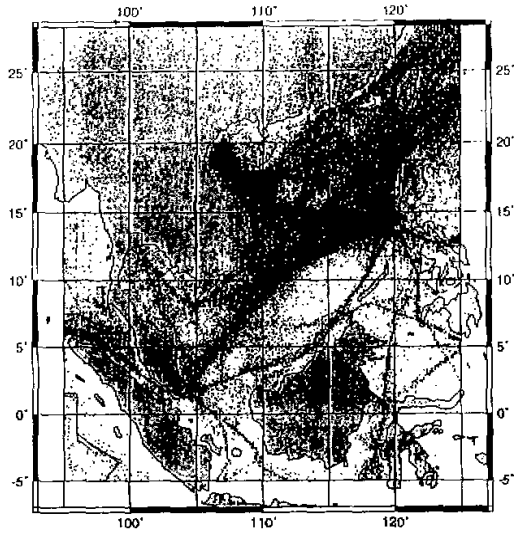

Fig. 2. Spatial distribution of MOODS stations for 1964–1984.

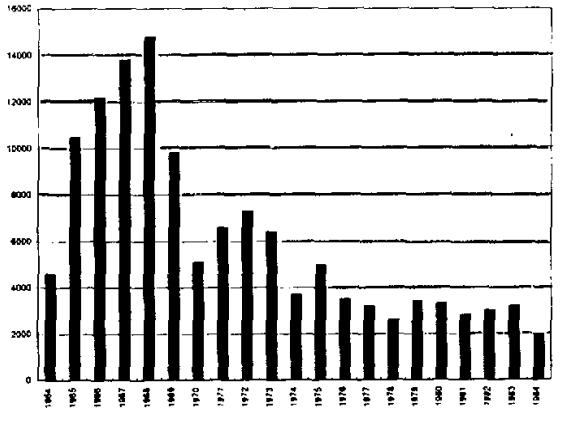

Fig. 3. Temporal distribution of MOODS stations during 1964–1984.

tions in different years, the seasonal variation within each year is not profound.

The main limitation of the MOODS data is its irregular distribution in time and space. Certain periods and areas are over sampled while others lack enough observations to gain any meaningful insights. Vertical resolution and data quality are also highly variable depending much on instrument type and sampling expertise. There are two data sparse areas in the SCS: Sunda Shelf and the western coastal region of Borneo (Figure 2). There are also frequent extended data gaps lasting 10–20 days during which no observation is taken any where in the SCS. In this study we carefully examined these spatial and temporal irregularities and selected the Spring of 1966 as the best period for our analysis.

Our 10-day interval data set is distributed evenly in time but unevenly in space. Before the hand analysis, we used an optimum interpolation (Gandin, 1963) to obtain a "first guess" to guide the hand analysis. The monthly sea-surface temperature (SST) climatology produced by Levitus (1982) was used as the mean field, and the optimum interpolation analyzes the departure of the observations from this mean field at the closest grid point, with a weight assigned to each observation that accounts for the variation in the spatial sampling. The data were then analyzed by hand with a subjective quality control based on both spatial and temporal continuities and the location of the original observations.

III. ANALYSIS OF THE SPRING 1966 SST DATA

The analyzed SST data from March-May 1966 are shown in Fig. 4. The evolution of the SST pattern may be described in the following sequence:

1. *Remnant of the Northern Winter Monsoon*

During March 1966 the SST was dominated by the basic meridional temperature gradient with cooler temperature to the north and northwest and warmer temperature to the south and southeast. This is basically the Northern winter pattern, except the SST in the northern SCS during the winter monsoon was cooler than March, with temperature often in

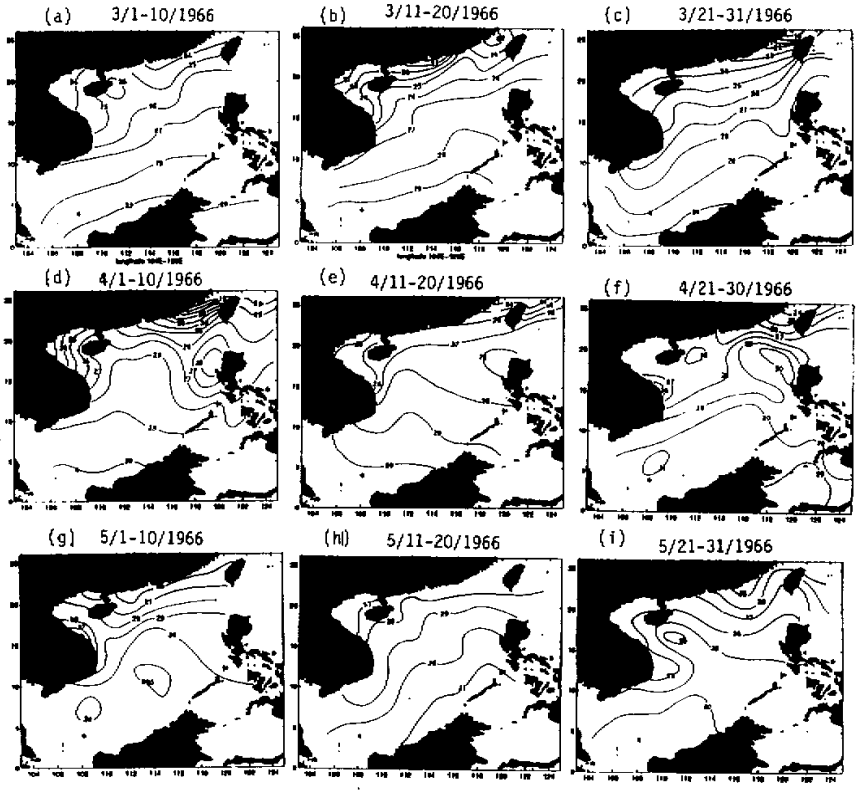

Fig. 4. Temporally varying sea surface temperature of the South China Sea from 1 March to 31 May, 1966.

the teens due to the effect of the northeasterly monsoon wind. There are minor fluctuations of the SST from one 10-day period to the next. For example, from early March to middle March (Figures 4a-b) the central SCS develops a slight warm tongue that intrudes from southeast (near Palawan) towards northwest (near Hainan) as indicated by the 26°-28°C isotherms. In late March (Figure 4c) SST in the Taiwan Strait was cooled by several degrees, apparently due to late-season freshening of northeasterlies. The northern SCS was somewhat affected with a slight cooling. Nevertheless, the northward bulge of the warm tongue represented by the 26°-28°C isotherms, now splits in two part, can still be observed. Figs. 4b-c also show a cooler region along the west coast of the Luzon Island. Due to lack of data, it is not clear whether this cooler region started in middle March (Figure 4b).

2. *Early Stage of the Warm-Core Eddy*

A warm core eddy begins to appear near the west coast of the Luzon Island in early April (Figure 4d). The eddy, with a size around 500,000 km^2, lasts through April and has a maximum temperature that increases from 28°to 30°C (Figures 4e-f). The warming occurs over nearly the entire SCS, with the highest SST observed in the southwestern SCS where the SST reaches 31°C. In the Taiwan Strait the cool SST that occurred in late March totally disappeared by mid-April. There is, however, some remnant of cool water in the Golf of Tonkin which left signals of small cool SST adjacent to the northeast middle Vietnam coast. The appearance of a cool eddy in late April (Figure 4f) may be related to this and the enclosed isotherms may be due to data coverage.

3. *Mature Stage of the Warm-Core Eddy*

The warm core eddy seems to expand and move southwestward during early May (Figure 4g), when the central and southern SCS was dominated by warm water (>30°C). The highest SST is observed in the region 111°E-116°E, 7°N-12°N, where a warm pool of >30.5°C is located. In the meantime, water near the eastern and southeastern coast of Vietnam begins to show a cooling tendency.

4. *Disappearing Stage of the Warm-Core Eddy*

The beginning of this period coincides with the onset of the Northern summer monsoon over the SCS. The SST during mid-May (Figure 4h) relaxed back to the ensemble mean pattern and the warm-core eddy disappears. The water surface temperature in the southeast SCS near northeastern Borneo and Palawan became reaching 31°C. Cold SST off the southeastern coast of Vietnam became more prominant with a clearly developed cool pool (SST<28°C) by late May (Figure 4i). This cool pool is most likely a result of the upwelling of cold water under the steady forcing of the southwest monsoon wind at the surface. Another cool pool appeared near the southeastern coast of China near Taiwan, with SST<25°C, apparently a result of the same monsoon forcing mechanism.

IV. POSSIBLE COMBINED WIND-BOTTOM TOPOGRAPHY EFFECTS DURING BOREAL SPRING

The life cycle of the warm-core eddy in the central SCS observed in 1966 shown in Figure 4 led us to propose an interpretation that is based on the topography and the surface wind. The bowl-type bottom topography shown in Figure 1 provides a favorable condition for the formation of eddies in the interior of the SCS. If the surface wind stress curl over the central SCS is anticyclonic, Ekman downwelling will occur in the central part of the "bowl" and Ekman upwelling will occur near the boundary of the "bowl" through mass balance. The downwelling prevents the deep cold water from advecting upward, and the upwelling helps

the deep cold water adveting upward. The downwelling process is favorable for the formation of warm pool and the upwelling is favorable for the cool pool.

From late winter to early spring, a surface anticyclone usually appears over the central SCS, as may be seen from the ensemble mean streamline analysis (Figure 5a, from Cheang, 1980). This anticyclone generates downwelling in the central SCS and in turn prevents the cold deep water from being advected to the surface. As spring starts the cold nrotheast monsoon diminishes and the sky over the SCS also enters a more clear period with less cloud cover and rainfall, and rapidly increasing solar radiative warming at the sea surface. The downwelling may effectively produce a warm pool in the central SCS, as is observed in Figure 4. This warm pool, with a temperature 1°C higher than the surroundings in a generally warm SCS, may lower the atmospheric surface pressure and promote the onset of the Northern summer monsoon. The appearance of a cyclonic circulation with the lower pressure after the onset (Figure 5b, from Cheang, 1980) may then generate Ekman upwelling in the central SCS, bringing the deep cold water into the surface mixed layer. This process may then destroy the warm-core eddy in the central SCS.

The above hypothesis is summarized in a flow chart shown in Figure 6. This hypothesis may be much too simplistic to represent the real annual cycle of the atmosphere and ocean interaction in the SCS, which is more complicated with many other factors and disturbances involved. There are also unknowns due to lack of data. Nevertheless, certain aspects of the hypothesis suggested in Figure 6 may be evaluated with a numerical model. In the next section, we will use a numerical model to test the first half of this hypothesis–the development of a warm-core eddy through the anticyclonic forcing at the surface and the resultant downwelling. This part of the hypothesis occurs in the Northern Spring, which is a period during which the SCS is relatively free from influences of external disturbances, such as the winter cold surge or the summer and fall tropical cyclones.

V. SIMULATION WITH A PRIMITIVE EQUATION MODEL

1. *Model Description*

The numerical model used to investigate the formation of the central SCS warm-core eddy is the three-dimensional model developed by Blumberg and Mellor (1983, 1987) with the hydrostatic and Boussinesq approximations (Bryan, 1969) and has the following features: 1) horizontal curvilinear coordinates and an "Arakawa C" scheme (Arakawa and Lamb, 1977), 2) sigma coordinates in the vertical with realistic bathymetry, 3) a free surface, 4) a second-order turbulence closure model for the vertical viscosity (Mellor and Yamada, 1974, 1982), 5) horizontal diffusivity coefficients calculated by the Samagorinsky (1963) parameterization, and 6) split time steps for barotropic and baroclinic modes.

The model domain is 99°E–121°E, 3°S–25°N which includes the South China Sea and the Gulf of Thailand. With a 20 km horizontal resolution and 23 vertical sigma coordinate levels, the model dimension is $125 \times 162 \times 23$ grid points. The time step is 25 s for the external mode and 900 s for the internal modes. All depths less than 10 m in the domain are set to be 10 m in order to satisfy the constraint $H+\eta>0$, where H is the depth and η the surface elevation anomaly. In the Samagorinsky parameterization, a horizontal mixing coefficient with $C=0.1$ is used, which results in the horizontal viscosity ranging from 200 to 500 m^2s^{-1}. The background vertical mixing coefficient is 10^2s^{-1}(Blumberg and Mellor, 1983, 1987; Chu, et al., 1996).

2. *Lateral Boundary Conditions*

Several straits connect the SCS to the Pacific Ocean and surrounding seas. Some are very

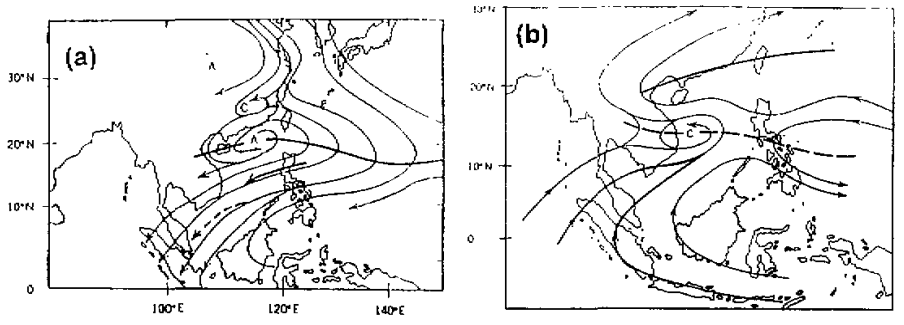

Fig. 5. Mean atmospheric surface streamline analysis for (a) winter, and (b) early spring (from Cheang, 1980).

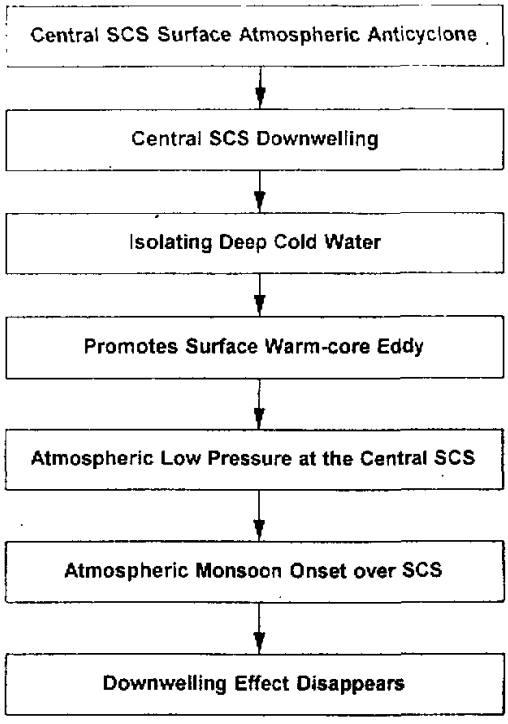

Fig. 6. A air–sea feedback mechanism for the formation and destruction of the central SCS warm-core eddy.

shallow (i.e., the Strait of Malacca) or irregular (i.e., the Balabac Strait), and are difficult to handle in a numerical model. Therefore, we close the Strait of Malacca, and all the small straits between Luzon Island and Borneo in the numerical model. We also combine the Karimata Strait and the Gasper Strait into one open boundary. After these treatments, our model has three open boundaries: northern boundary (Taiwan Strait), eastern boundary (Luzon Strait), and southern boundary (Karimata–Gasper Strait). The transports at the three

open boundaries are determined according to Wyrtki's (1961) estimation with some modification due to the boundary treatment. Table 1 shows the seasonal variation of the transport (1 sv $\equiv 10^6 m^3 s^{-1}$) at the three open boundaries. The summation of the total transport through the open boundaries is always zero in order to keep the mass conservation.

Table 1. The Bi-monthly Variation of Mass Transport (sv) at the Open Boundaries. The Values Were Taken from Wyrtki (1961).

Month	Feb.	Apr.	Jun.	Aug.	Oct.	Dec.
Gasper & Karimata Straits (Eastward Positive)	4.4	0.0	−4.0	−3.0	1.0	4.3
Luzon Strait (Eastward Positive)	−3.5	0.0	3.0	2.5	−0.6	−3.4
Formosa Strait (Northwards Positive)	−0.9	0.0	1.0	0.5	−0.4	−0.9

The barotropic velocity at the open boundaries (V_n^{BT}) is obtained by

$$V_n^{BT} = \frac{Transport}{\int_l Hdl}, \tag{1}$$

where l is the boundary width, and n means the normal direction to the boundary. The baroclinic velocity, $V_n^{BC}(\sigma)$ is calculated by

$$V_n^{BC}(\sigma) = V_n^{BT} \frac{e^{\sigma}}{1 - e^{-1}}. \tag{2}$$

During the numerical integration, both V_n^{BT} and V_n^{BC} are interpolated into the time step from the bi-monthly values of the volume transport listed in Table 1.

On the lateral open boundaries, temperature (T) and salinity (S) are prescribed at inflow boundaries, whereas at outflow boundaries, the advection equation, namely,

$$\frac{\partial}{\partial t}(T,S) + V_n \frac{\partial}{\partial n}(T,S) = 0 \tag{3}$$

is solved from both barotropic and baroclinic modes.

3. *Surface Forcing*

The atmospheric forcing includes wind forcing and thermodynamic forcing. The monthly mean climatological wind stress data set (Hellerman and Rosenstein, 1983) is used as the wind data for the middle of the month. The data are then interpolated to give daily values and interpolated them on each day. The wind stress has a typical magnitude of 1 dyne / cm^2 (corresponding to surface wind speed 10 m / s). Northeasterly winds dominate during the Northern winter monsoon, and southwesterly winds prevail during the Northern summer monsoon. The wind stress field is referred to as the climatological wind forcing.

There are two approaches setting up surface thermal forcing: 1) flux forcing when the surface heat and salt fluxes, Q_H(W m^{-2}) and Q_S(m s^{-1}) are given, and 2) restoring forcing when the fluxes are not given and the model surface temperature (T) and salinity (S) are relaxed to the observed values (T_{ob}) and (S_{ob}):

$$K_H \frac{\partial T}{\partial z} = \alpha_1 \frac{Q_H}{\rho c_p} + \alpha_2 C(T_{ob} - T),$$

$$K_H \frac{\partial S}{\partial z} = \alpha_1 Q_S + \alpha_2 C(S_{ob} - S). \tag{4}$$

Here K_H is the thermal exchange coefficient and C is the relaxation constant taken to be 0.7 m / d, which is equivalent to a relaxation time of 43 days for an upper layer of 30 m thick. The coefficients α_1,α_2, are (0,1)-type switcher parameters: when $\alpha_1=1$, $\alpha_2=0$, we only have the flux forcing; when $\alpha_1=0$, $\alpha_2=1$, we only have the restoring forcing, when $\alpha_1=1$, $\alpha_2=1$, we have both the flux forcing and the restoring forcing. In this simulation we only use the restoring forcing as the surface thermal forcing. We construct the (T_{ob},S_{ob}) data through interpolation from the climatotological monthly mean temperature and salinity data (Levitus, 1982). The climatological (T,S) data have different horizontal and vertical resolutions from our model, and are converted into our model grids by the optimal interpolation (OI).

4. *Simulation Results*

The model is initiated from the April mean fields (Levitus, 1982) and forced by the surface wind stress (Hellerman and Rosenstein, 1983) and thermodynamic fluxes as depicted in (4). Both the surface forcing and the transport at the open boundaries are interpolated in time to give daily values. The total integration time is three years, during which the annual climatological forcing is repeated for three cycles. The third year's output is considered the quasi-equilibrium result, and the end of each month of this third year will be used to represent each respective month in the discussion.

In Figure 7 the sea temperatures at 5 m for March 30, April 30, May 30 and June 30 are displayed. A distinctive feature in the sea temperature is the warm-core region in the eastern central SCS in all months shown. For March, the highest temperature area of this warm core is enclosed by a 30°C isotherm. After one month, the temperature of this warm core increases by nearly 2°C. This can be seen by the area enclosed by the 31°C isotherm in the April diagram which roughly replaces the area enclosed by the 29°C isotherm in March. Also, the maximum temperature in April occurs in a small area of warmer than 32°C. This warming trend continues into May with an increase of approximately 1°C, but appears to stop after May. The June temperature pattern has about the same maximum temperature as May, but the core structure become less organized, indicating that the development stage of the warm-core eddy is over.

Corresponding to Figure 7, the flows at 5 m for March 30, April 30, May 30 and June 30 are shown in Figure 8. Although there are several eddy scale features shown in these diagrams, most of the general rotation directions for the northern and central SCS are clearly anticyclonic starting from March. This anticyclonic vorticity is a result of the seasonal atmospheric surface forcing. The net anticyclonic rotation persists through May, with the locally cyclonic regions mostly showing smaller vorticity magnitudes compared to the anticyclonic regions. Thus, the warming of the upper ocean in the central-eastern SCS is consistent with the persistence of anticyclonic flow. For June, the dominance of the anticyclonic circulations begins to decline, with several areas in the central and eastern SCS showing significant cyclonically-rotating eddies. This development of cyclonic flow occurs as a result of the development of the Northern summer monsoon trough in the surface climatology. It corresponds to the termination of the upper ocean warming trend, and is consistent with the concept that the thermal field is largely influenced by the atmospheric forcing through the Ekman process.

VI. CONCLUDING REMARKS

Subjective analysis of the MOODS data during the first six months of 1966, binned for three 10-day periods each month, allowed us to identify the development of a warm-core eddy in the central SCS during northern Spring. The maximum SST of this eddy reached 30°C

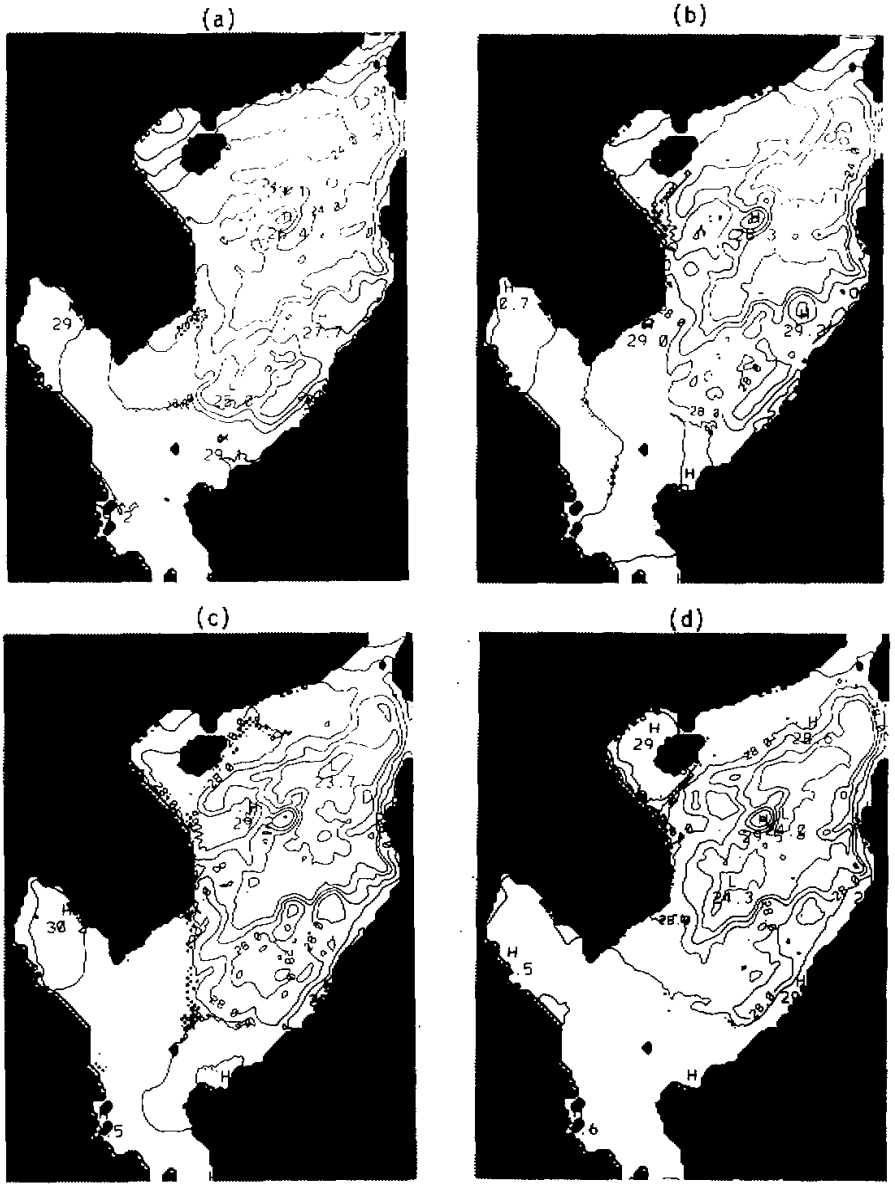

Fig. 7. Model simulated SST for (a) 30 March, (b) 30 April, (c) 30 May, and (d) 30 June.

and higher, implying significant latent and sensible heat fluxes into the lower levels of the atmosphere. This is the period immediately before the onset of the Northern summer monsoon over the SCS, and we postulated on the possibility that the development of this warm pool may play an important role in the monsoon development. Firstly, the warm pool may be a result of both the radiative warming under clear sky and the downwelling driven by a

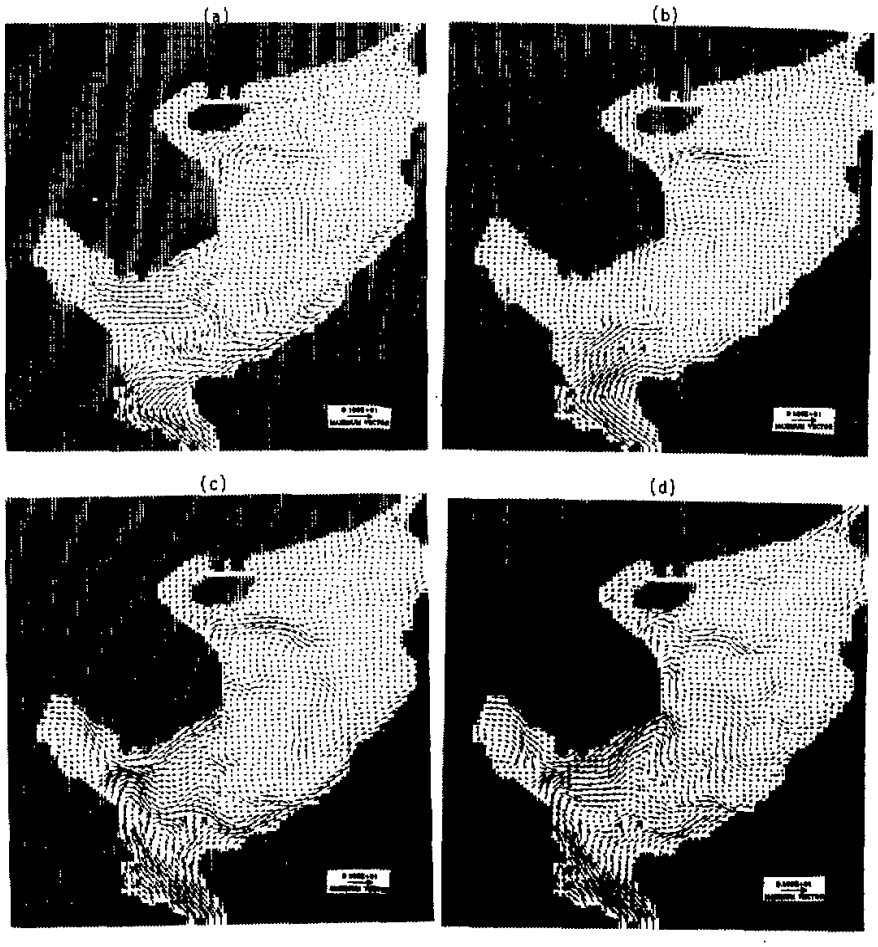

Fig. 8. Model simulated surface circulations for (a) 30 March, (b) 30 April, (c) 30 May, and (d) 30 June.

climatological anticyclone at the surface. Its existence, in turn, will help the lowering of the atmospheric surface pressure, which is favorable to the seasonal transiction from the Northern winter anticyclone to the Northern summer cyclone or monsoon trough. A numerical model was used to test this hypothesis of the atmosphere–ocean interaction in the SCS.

The numerical simulation was meant to demonstrate the possibility that an upper warm-core eddy in the general neighborhood of the eastern SCS can be developed during the boreal spring and has a seasonal evolution that approximately give warming through May and cooling afterwards. These thermal changes correspond to a net enhancement of anticyclonic flow through May and a net weakening into June. Thus, the basic premises of our hypothesis are simulated, although the magnitude of warm core is too high. The model was limited by the exclusion of several important processes in the atmosphere and ocean. For example, during Northern summer, the monsoon should bring significant rainfall that will cool the SCS and dampen the warm pool. Occurrences of tropical cyclones and other tropical disturbances will also significantly change the state of the atmosphere and the upper ocean.

These processes are not included in the model so we are unable to simulate the decaying process after the warm-core eddies developed. Furthermore, interannual variations in both the atmosphere and the ocean are prominent in the tropical monsoon region. Our data analysis is limited to 1966 only, it is not known how frequent the Northern spring warm-core eddy appears in other years. The numerical simulation is based on the forcing of the mean climatological annual cycle, variations from one year to another are almost certain to change certain aspects of the simulation results.

Authors are grateful to Yongfu Qian and Shihua Lu for discussion. This work was supported by the Office of Naval Research NOMP AND NAMP Programs, and by the Naval Oceanographic Office.

REFERENCES

Arakawa, A. and V.R. Lamb (1977), Computational design of the basic dynamical processes of the UCLA general circulation model, *Methods in Computational Physics*, Academic Press, New York, **17**: 119-143.

Blumberg, A.F and G.L. Mellor (1978), A description of a three-dimensional coastal ocean circulation model, *In: Three Dimensional Coastal Ocean Models* (Edited by N.S. Heaps), American Geophysical Union, 1-16.

Cheang, B.K. (1980), Some aspects of winter monsoon and its characteristics in Malaysia, Research Publication No. 2, Maylaysian Meteorological Service.

Chu, P.C., M.J. Huang and E.X. Fu (1996), Formation of the South China Sea warm-core eddy in boreal spring, *Proceedings, Symposium on the Global Ocean-Atmosphere-Land System (GOALS)*, American Meteorological Society, Boston, 155-159.

Dale, W.L. (1959), Winds and drift currents in the South China Sea, *Malayan Journal of Tropical Geography*, **8**: 1-31.

Gandin, L.S. (1965), Objective analysis of meteorological fields, Israel Program for Scientific Translation, 242pp.

Hellerman, S. and M. Rosenstein (1983), Normal monthly wind stress over the world ocean with error estimates, *Journal of Physical Oceanography*, **13**: 1093-1104.

Levitus, S. (1982), Climatological atlas of the world ocean, NOAA Professional Paper, 13, U.S. Government Printing Office, Washington D.C..

Mellor, G.L. and T. Yamada (1974), A hierarchy of turbulence closure models for planetary boundary layer, *Journal of Atmospheric Sciences*, **31**: 1791-1796.

Mellor, G.L. and T. Yamada (1982), Development of a turbulence closure model for geophysical fluid problems, *Reviews of Geophysics and Space Physics*, **20**: 851-875.

Nitain, H. (1970), Oceanographic conditons in the sea east of Philippines and Luzon Strait in summer of 1965 and 1966, *In: The Kuroshio-A Symposium on Japan Current* (J.D. Marr edited), East-West Press, Honolulu, 213-232.

SCSIO (South China Sea Institute of Oceanology, Academia Sinica) (1985), Integrated investigation report on sea area of the South China Sea (II), Science Press, Beijing, 183-231.

Smagorinsky, J (1963), General circulation experiments with the primitive equations, *Monthly Weather Reviews*, **91**: 99-164.

Soong, Y.S., J.H. Hu, C.R. Ho, and P.P. Niiler (1995), Cold-core eddy detected in South China Sea, *EOS*, 345-347.

Uda, M. and T. Nakao (1972), Water masses and currents in the South China Sea and their seasonal changes, *In: The Kuroshio-Proceedings of the 3rd CSK Symposium, Bangkok*, Thailand, 161-188.

Wyrtki, K. (1961), Scientific results of marine investigations of the South China Sea and Gulf of Thailand 1959-1961, NAGA Report 2.